Eur. Phys. J. B **6**, 25–32 (1998)

THE EUROPEAN PHYSICAL JOURNAL B

Al-Cu approximants in the Al_3Cu_4 alloy*

C. Dong[1,2,3,a], Q.H. Zhang[2], D.H. Wang[2], and Y.M. Wang[2]

[1] State Key Laboratory for Materials Modification by Laser, Ion and Electron Beams, Dalian University Technology, Dalian, 116024, P.R. China
[2] Department of Materials Engineering, Dalian University of Technology, Dalian 116024, P.R. China
[3] Atomic Imaging of Solids, Institute of Metals Research, Academia Sinica, Shenyang 110015, P.R. China

Received: 8 July 1997 / Revised: 19 May 1998 / Accepted: 16 June 1998

Abstract. The Al_3Cu_4 composition, with an e/a ratio of 1.86 being close to ternary Al-Cu-TM (Transition Metal) quasicrystals, has been chosen for the search of Al-Cu approximants. Phase structures and compositions were studied using TEM, X-ray diffraction and EPMA techniques. Two new phases were found: face-centered orthorhombic oF-$Al_{43.2}Cu_{56.8}$ ($a = 0.816_6$, $b = 1.414_9$, $c = 0.999_5$ nm) and body-centered orthorhombic oI-$Al_{41.3}Cu_{58.7}$ (oI, $a = 0.408_3$, $b = 0.707_4$, $c = 0.999_5$ nm). Their e/a ratios are the same as that of the Al-Cu-Fe icosahedral quasicrystal. Their space groups are probably oF-Fmm2 and oI-Imm2. Both are B2 vacancy-containing superstructures; unit cell compositions can be expressed approximately as oF-$Al_{36}Cu_{48}\square_{12}$ and oI-$Al_8Cu_{12}\square_4$ ($\square$: vacancies). They both exist in twinning variants of the types 120°/[001] and 180°/[310]. Such twinning modes indicate that these orthorhombic phases are the decomposition products of a high-temperature parent phase $\varepsilon 2$-Al_2Cu_3, the atomic structure of which contains pentagonal atomic arrangements. Therefore the oF, oI, and $\varepsilon 2$ phases are all B2-based approximants corresponding to the Al-Cu-TM quasicrystals.

PACS. 61.44.+p Semi-periodic solids – 61.66.Dk Alloys

1 Introduction

Quasicrystals mainly exist in Al-based alloy systems [1]. Among the Al-based systems, ternary Al-Cu-TM (Transition Metal) systems are of particular importance because some of these quasicrystals are stable phases [2]. In the binary alloy systems constituting the ternary Al-Cu-TM systems, many metastable quasicrystals have been found in Al-rich Al-TM systems, but little has been done so far in the Al-Cu system. The latter issue has been addressed only recently [3–6] because the only Al-rich Al-Cu phase is the non-approximant Al_2Cu phase. It is now a well-known fact that quasicrystals and their approximants are Hume-Rothery phases having similar valence electron concentrations [7]. Since these phases are located near a straight line with a constant e/a ratio in an Al-Cu-TM ternary phase diagram, they are termed e/a-constant phases. For example, there are at least three such phases in the Al-Cu-Fe system, namely monoclinic λ-$Al_{13}Fe_4$, icosahedral quasicrystal $Al_{62.3}Cu_{24.9}Fe_{12.8}$ (i-AlCuFe), and hexagonal ϕ-$Al_{10}Cu_{10}Fe$ (Al_3Ni_2 type). This new understanding of the approximant concept based on valence electron concentration correspondence [8] sheds light on the research on Al-Cu approximants: these approximants should also be e/a-constant phases. Two new orthorhombic Al-Cu phases oF and oI were thus discovered in an $Al_{43}Cu_{57}$ alloy with $e/a = 1.86$ [3]. The present paper gives a detailed account of their strctural investigation in order to clarify their approximant nature.

2 Review of Al-Cu phases

Although the Al-Cu phase diagram has been an object of intense investigation (refer to Ref. [9] for a general review of the Al-Cu system), the part of the phase diagram near the region of 50 ∼ 70 at% Cu is not well understood and most of the phase structures are unknown. In Table 1 are listed phase symbols, compositions, and structural data of Cu-rich Al-Cu phases. Only three phases $\eta 1$, $\varepsilon 2$, and $\gamma 1$ are completely known. The latter two phases are the concern of the present study.

The $\varepsilon 2-Al_2Cu_3$ phase is hexagonal with parameters $a = 0.4146$ nm, $c = 0.5063$ nm [10]. Its space group is P63/mmc. It is a B2-superstructure with a partially occupied NiAs structural type. There are three types of atomic positions: Cu atoms completely occupying (0,0,0), Cu atoms partially occupying (1/3, 2/3, 3/4) with an occupancy of 0.7, and Al atoms completely occupying (1/3, 2/3, 1/4). Our sample's nominal composition Al_3Cu_4 is situated within the $\varepsilon 2$'s composition range 55.0 ∼ 61.1 at% Cu. Since $\varepsilon 2$ is a high-temperature stable phase, the phases in our as-cast sample might be its decomposition

* Supported by the National Natural Science foundation of China under the grant n° 59525103.

[a] e-mail: dong@dlut.edu.cn or mmlab@dlut.edu.cn

Table 1. Structural data of the Cu-rich Al-Cu phases. The atomic structures of the phase marked with * are reported in *Pearson's Handbook of Crystallographic Data for Intermetallic Phases* [13]. The phase symbols are adopted from reference [14].

symbol	at% Cu	crystallographic data, lattice constants are in nm
$^*\eta 1$	49.8 ∼ 52.4	oP16, Pban, 0.410, 1.2024, 0.865
	49.8 ∼ 52.4	oC16, Cmmm, 0.410, 1.2024, 0.865
$\eta 2$	49.8 ∼ 52.3	mC20, C2/m, 1.2066, 0.4105, 0.6913, $\beta = 55.04°$
$\zeta 1$	55.2 ∼ 59.8	hP42, P6/mmm, 0.810, 1.000
	55.5	hP42, P6/mmm, 0.810, 1.237
$\zeta 2$	55.2 ∼ 56.3	monoclinic (?), 0.707, 0.408, 1.002, $\beta = 90.63°$
$\varepsilon 1$	59.4 ∼ 62.1	cubic (?),
$^*\varepsilon 2$	55.0 ∼ 61.1	hP4, $B8_1$, $P6_3/mmc$, NiAs type, 0.4146, 0.5063
δ	59.3 ∼ 61.9	rhombohedral, R3m, R-type γ-brass,
γ_0	59.8 ∼ 69	
$^*\gamma_1$	62.5 ∼ 69	cP52, $D8_3$, $P\bar{4}3m$, P-type γ-brass (Al_4Cu_9 type), 8.7068
β_0	67.6 ∼ 70.2	
β	70.6 ∼ 82.0	cI2, A2, Im3m, W type, 0.29584 (at 672 °C)
	75.7	cI2, A2, Im3m, W type, 0.2946 (at 580 °C)
γ'		DO_{19}, Pmmm, Cu_3Ti type, 0.451, 0.520, 0.422
α_2	76.5 ∼ 78	DO_{22}, 0.3666, 0.3675

products. Such solid-state phase transitions must impose a particular influence over the twinning modes of the oF and oI phases.

The atomic structure of the simple-cubic $\gamma 1 - Al_4Cu_9$ phase was resolved by Bradley and Jones [11], who noted its structural similarity with γ-brass. It was therefore termed P-type γ-brass. In this paper we use symbol γ to represent this phase. This structure can be described by clusters of 26 atoms located on a body-centered cubic lattice. One Al_4Cu_9 cell ($a = 0.87068$ nm for a single-crystal specimen with the $Al_{31.9}Cu_{68.1}$ composition [12]) contains 27 CsCl-type pseudocells with two atomic sites being vacant. As discussed in our previous paper [6], although its typical e/a ratio of 1.62 is far from that of the i-AlCuFe, its valence electron concentration per unit volume is nearly the same as that of the i-AlCuFe phase. So it can be considered as an approximant according to the new criterion. Its atomic structure is also closely related to that of quasicrystals. One unit cell consists of two kinds of layers, flat and puckered, that are stacked along a $\langle 110 \rangle$ direction corresponding to the 5(10)-fold axes of quasicrystals. Both the stacking sequence and the periodicity resemble those of the decagonal Al-Mn phase. Moreover, atoms tend to form pentagons around vacancy sites and these pentagons are aligned into pentagonal columns. The δ and γ_0 phases, with their compositions being closer to that of our sample than the γ phase is, have deformed γ-brass structures, but their exact atomic structures are still unknown.

3 TEM and X-ray diffraction: experiments and results

Ingots of the $Al_{43}Cu_{57}$ composition, whose e/a ratio is close to that of the i-AlCuFe phase, were prepared by arc melting of pure metals under an Ar atmosphere. The as-cast samples were annealed at 500 °C for 10 hours and cooled slowly in furnace. Transmission electron microscopy (TEM), X-ray diffraction, and electron probe microanalysis (EPMA) were used to characterize the phases. Orientation relationships (ORs) between variants of two new orthorhombic phases oF (Face-centered) and oI (body-centered) are frequently used to reveal structural correspondence. See Appendix for more details about the OR calculations.

In contrary to the established phase diagram [9], two new phases have been observed in both as-cast and annealed Al_3Cu_4 samples: face-centered orthorhombic phase oF with $a_{oF} = 0.8166$ nm, $b_{oF} = 1.4149$ nm, $c_{oF} = 0.9995$ nm, and body-centered orthorhombic phase oI with $a_{oI} = 0.4083$ nm, $a_{oI} = 0.7074$ nm, $c_{oI} = 0.9995$ nm [3]. The lattice parameters were refined from X-ray powder diffraction data reported in Table 2. The lattice constants satisfy special ratios a_{oF}: b_{oF}: $c_{oF} \approx 1/\sqrt{12} : 1/2 : 1/\sqrt{2}$, a_{oI}: a_{oI}: $c_{oI} \approx 1/\sqrt{3} : 1 : 1/\sqrt{2}$, leading to the following relationships linking plane indices (hkl) and its normal directional indices $[uvw]$: $h : k : l \approx 2u : 3v : 3w$ for oF and $h : k : l \approx u : 3v : 6w$ for oI. Due to these special relationships, the two phases are quite similar in diffraction features and are difficult to distinguish from each other. We have carried out a double-tilting experiment in TEM and have obtained Selected Area Electron Diffraction (SAED) patterns along different zone axis in order to determine their lattice structures. Two sets of SAED patterns, one for oF and another for oI, are presented in Figure 1 and Figure 2.

The as-cast sample contains a mixture of oF, oI, and a minute amount of γ-Al_4Cu_9, the oI phase being the major phase. After the annealing at 500 °C for 10 hours, γ-Al_4Cu_9 disappears and the major phase in the sample

Table 2. Indexing of the X-ray diffraction pattern of the powdered as-cast $Al_{43}Cu_{57}$ sample (wave length 0.15405 nm) using the face-centered orthorhombic oF-$Al_{43.2}Cu_{56.8}$ and body-centered oI-$Al_{41.3}Cu_{58.7}$ phase. The intensity data (I) is represented by relative peak height, the lattice spacing D in nm, and 2θ angle in degrees.

measured data			oF, 0.816_6, 1.414_9, 0.999_5						oI, 0.408_3, 0.707_4, 0.999_5					
$2\theta^\circ$	D	I	h	k	l	$2\theta^\circ$	D	I	h	k	l	$2\theta^\circ$	D	I
15.4	0.576	4	1	1	1	15.33	0.5773		0	1	1	15.33	0.5773	4
21.8	0.407	3	2	0	0	21.75	0.4082	4						
			0	2	2	21.75	0.4082							
23.4	0.380	7	1	3	1	23.52	0.3781		1	0	1	23.52	0.378	6
25.1	0.354	12	0	4	0	25.16	0.3537	11	0	2	0	25.16	0.3537	11
			2	2	0	25.16	0.3536	21	1	1	0	25.16	0.3537	21
26.6	0.335	1												
29.6	0.302	2	1	1	3	29.62	0.3014		0	1	3	25.62	3.014	1
29.8	0.300	3												
30.1	0.297	1												
30.6	0.292	1												
31.0	0.289	8	0	4	2	30.95	0.2887		0	2	2	30.95	0.2887	
			2	2	2	30.95	0.2887		1	1	2	30.95	0.2887	
34.8	0.258	3	1	5	1	34.70	0.2583		1	2	1	34.70	0.2583	1
			3	1	1	34.71	0.2582		1	0	3	34.72	0.2581	2
			1	3	3	34.71	0.2582							
39.4	0.229	6	3	3	1	39.22	0.2295		0	3	1	39.23	0.2295	1
43.4	0.208	21	1	5	3	43.36	0.2085		1	2	3	43.35	0.2085	1
			3	1	3	43.36	0.2085							
44.3	0.204	100	2	6	0	44.33	0.2042	92	1	3	0	44.32	0.2042	92
			4	0	0	44.33	0.2041	46	2	0	0	44.33	0.2042	46
			0	4	4	44.33	0.2041	50	0	2	4	44.34	0.2041	50
			2	2	4	44.33	0.2041	100	1	1	4	44.35	0.2041	100
47.0	0.193	3	4	2	0	46.24	0.1961		0	3	3	47.17	0.1925	1
			3	5	1	47.16	0.1925		2	1	1	47.17	0.1925	
			1	7	1	47.16	0.1925		0	1	5	47.17	0.1924	
			3	3	3	47.18	0.1924							
			1	1	5	47.18	0.1924							
50.8	0.180	1	1	3	5	50.81	0.1795		1	0	5	50.82	0.1795	1
51.8	0.176	1	0	8	0	51.64	0.1769	1	0	4	0	51.64	0.1769	1
			4	4	0	51.65	0.1768	3	2	2	0	51.65	0.1768	3
57.7	0.160	1	3	7	1	57.48	0.1602		1	4	1	57.48	0.1602	
			5	1	1	57.50	0.1601		1	2	5	57.50	0.1601	
			1	5	5	57.51	0.1601		1	3	4	58.30	0.1581	
			3	1	5	57.51	0.1601		2	0	4	58.32	0.1581	
60.8	0.152	3	2	0	6	59.92	0.1542	1	2	3	1	60.66	0.1525	1
			1	9	1	60.64	0.1526		0	3	5	60.68	0.1525	
			5	3	1	60.66	0.1525		0	2	6	61.48	0.1507	
			3	3	5	60.70	0.1525		1	1	6	61.48	0.1507	
			0	4	6	61.48	0.1507							
			2	2	6	61.48	0.1507							
64.5	0.144	13	0	8	4	64.50	0.1444	15	0	4	4	64.49	0.1444	15
			4	4	4	64.50	0.1443	30	2	2	4	64.50	0.1443	30
65.0	0.143	9												
65.4	0.143	1	3	0	6	65.72	0.1421							
66.5	0.141	1	0	10	0	65.96	0.1415		0	5	1	66.72	0.1401	
			2	4	6	66.02	0.1414		2	3	3	66.73	0.1400	
			1	9	3	66.72	.1401		2	1	5	66.76	0.1400	
			5	5	1	66.73	0.1401		0	1	7	66.78	0.1400	
			5	3	3	66.74	0.1400							
			1	7	5	66.74	0.1400							
			3	5	5	66.75	0.1400							
			1	1	7	66.77	0.1400							

Table 2. (Continued)

73.5	0.129	1	2	10	2	73.23	0.1291	1	0	5	3	72.52	0.1301	
			4	8	2	73.23	0.1291		1	5	2	73.23	0.1291	
			6	2	2	73.25	0.1291		2	4	2	73.25	0.1291	
			2	6	6	73.27	0.1291		3	1	2	73.27	0.1291	
			4	0	6	73.27	0.1291		1	3	6	73.27	0.1291	
									2	0	6	73.27	0.1291	
75.6	0.126	1	1	1	1	75.35	0.1260	1	3	2	1	75.35	0.1260	
			5	7	1	75.35	0.1260	1	1	4	5	75.38	0.1260	
			3	9	3	75.35	0.1260		3	0	3	75.38	0.1260	
			3	7	5	75.37	0.1260		1	2	7	75.40	0.1259	
			5	1	5	75.39	0.1260							
			1	5	7	75.40	0.1260							
			3	1	7	75.41	0.1259							

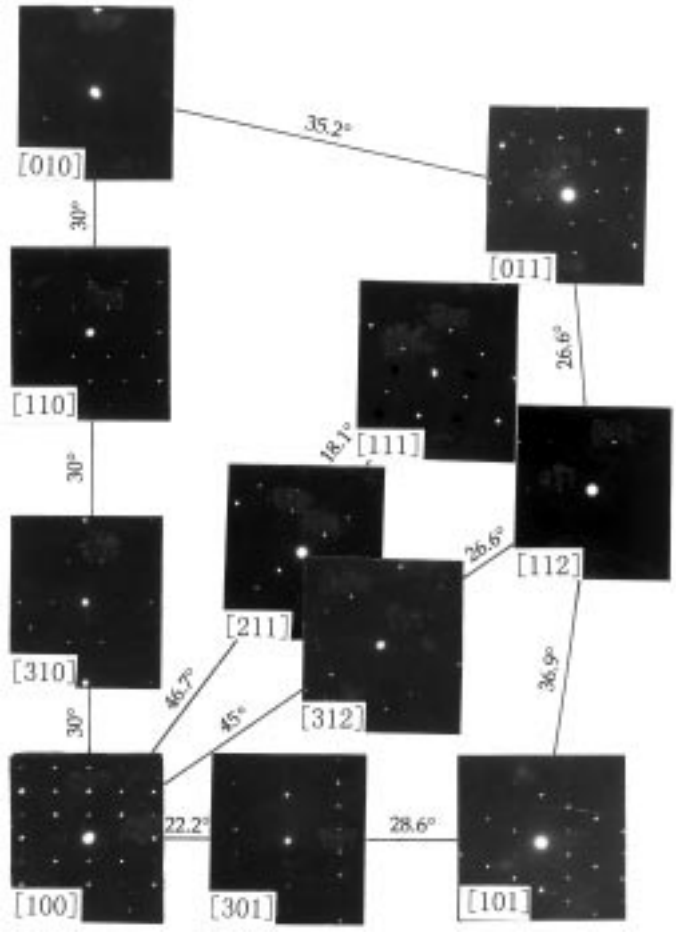

Fig. 1. SAED patterns arranged in a stereo manner for the oF phase.

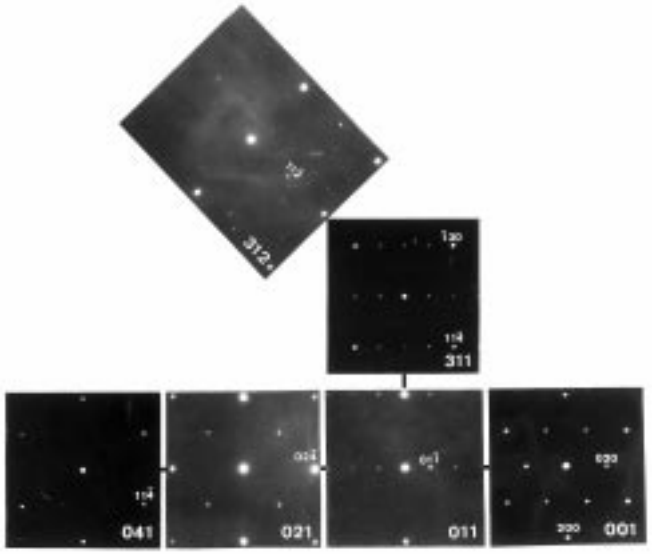

Fig. 2. SAED patterns arranged in a stereo manner for the oI phase.

turns to oF, indicating a phase transition from γ and oI to oF. The compositions of oF, oI, and γ are $Al_{43.2}Cu_{56.8}$, $Al_{41.3}Cu_{58.7}$, and $Al_{39.6}Cu_{60.4}$ respectively according to EPMA measurements.

The oF phase is always twinned. Figure 3 shows four important SAED patterns of the oF phase. There are two $[001]_{oF}$ variants in Figure 3a that are related to each other by a 60° rotation along $[001]_{oF}$. This is a 3-fold or a 6-fold twining. Figure 3b is a composite pattern of $t1$-$[010]_{oF}$ (spots of which are indicated by arrows and the (200) and (002) spots are indexed) and $t2$-$[310]_{oF}$ (its $(\bar{1}3\bar{1})$ and $(00\bar{2})$ spots are indexed). The corresponding OR matrix between these two variants $\begin{bmatrix} 1/2 & 3/4 & 0 \\ -1/2 & 1/2 & 0 \\ 0 & 0 & 1 \end{bmatrix}$ gives $60°/[001]_{oF}$, in confirmation of Figure 3a. Figures 3c and 3d are taken from two adjacent oF variants, the OR in this case being expressed by matrix $\begin{bmatrix} 1/2 & -3/2 & 0 \\ 1/2 & 1/2 & 0 \\ 0 & 0 & 1 \end{bmatrix}$ ($t1$-$[100]_{oF}$, $t2$-$[110]_{oF}$). Again, the 3- or 6-fold twinning mode is confirmed. We will see later that the twinning mode in real space is of 3-fold type.

Figure 4a shows a SAED pattern of another type of twinning mode. This pattern contains diffraction spots from two $[112]_{oF}$-orientated variants illustrated in Figure 4c, the twinning mode being 2-fold with the OR matrix $\begin{bmatrix} 1/2 & -3/4 & 0 \\ -1/2 & -1/2 & 0 \\ 0 & 0 & -1 \end{bmatrix}$, or $180°/[310]_{oF}$. Note that this

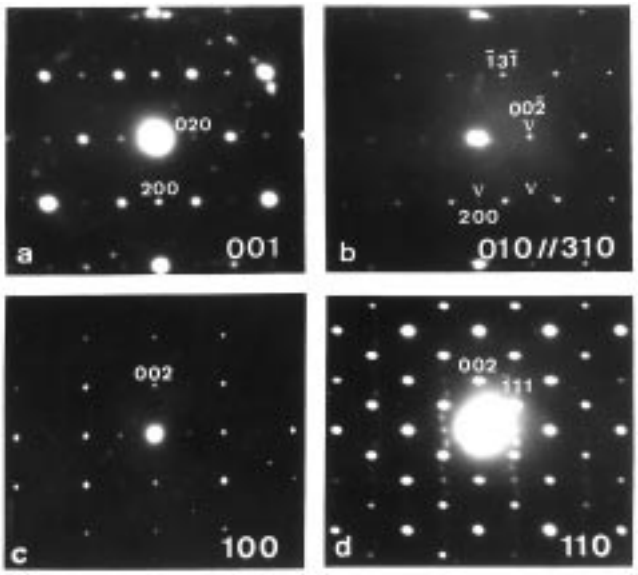

Fig. 3. SAED patterns of the oF phase showing the 3- or 6-fold twinning with twinning axis $[001]_{oF}$. In (a) there are two $[001]_{oF}$ variants rotated with respect to each other by 60°. Figure 3b contains reflections from two zone axes, three arrowed reflections being from the $[010]_{oF}$ zone axis and two indexed ones ($\bar{1}3\bar{1}$) and ($00\bar{2}$) from the $[310]_{oF}$ zone axis. Figures 3c and 2d are parallel patterns.

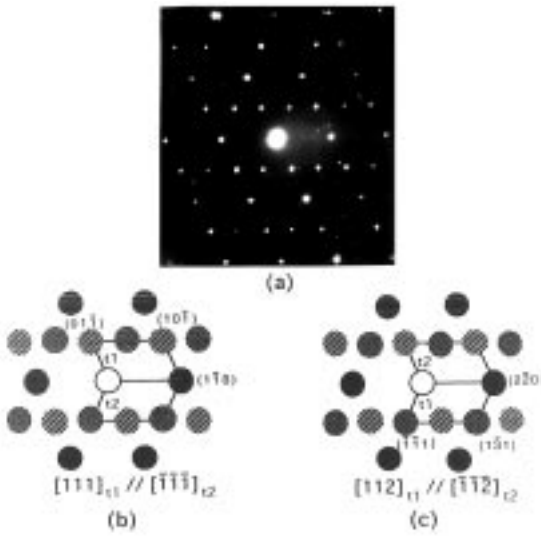

Fig. 4. 2-fold twinning SAED pattern (a) that can either be indexed as $[111]_{oI}$ (b) or $[112]_{oF}$ (c).

two-fold twinning axis $[310]_{oF}$ is perpendicular to the 3- or 6-fold $[001]_{oF}$ axis.

Though some spots are quite weak (for example $(020)_{oF}$ spot in Fig. 3a), there is no special extinction rule. Therefore, three space groups are possible for the oF phase: Fmm2, Fmmm and F222.

This phase must have a close structural relationship with the hexagonal $\zeta 1$ (55.2 $\sim$ 59.8 at% Cu) phase, noting that $a_{\zeta 1} = 0.810$ nm $\approx a_{oF}$ and $c_{\zeta 1} = 1.000$ nm $\approx c_{oF}$. Omitting some weak reflections such as $(020)_{oF}$

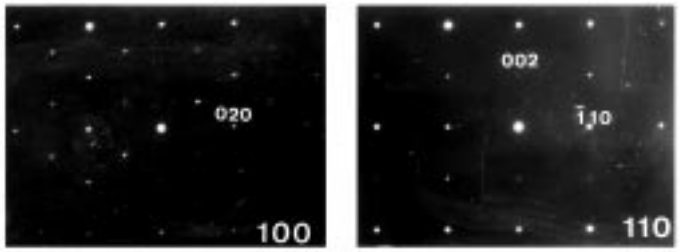

(a) (b)

Fig. 5. Two parallel patterns $[100]_{oI}$ and $[110]_{oI}$ reflecting 6-fold twinning $60°/[001]_{oI}$ in reciprocal space.

orthorhombic oF can transform to hexagonal $\zeta 1$ (Fig. 3a would be hexagonal).

The oI phase exists in similar twinning modes. Figure 5 shows two parallel SAED patterns $t1$-$[100]_{oI}$ and $t2$-$[110]_{oI}$ taken from two adjacent oI variants. The OR matrix is $\begin{bmatrix} 1/2 & 3/2 & 0 \\ 1/2 & 1/2 & 0 \\ 0 & 0 & 1 \end{bmatrix}$, signifying a 6-fold or 3-fold twinning $60°/[001]_{oI}$. The SAED pattern in Figure 4a can also be indexed as $[111]_{oI}$ in Figure 4b and the corresponding twinning mode is a 2-fold twinning $180°/[310]_{oI}$. Again the twinning axes $[001]_{oI}$ (6-fold or 3-fold) and $[310]_{oI}$ (2-fold) are perpendicular to each other.

No special distinction rule is found so that the oI space group must be one of the three possibilities: Imm2, I222 and Immm.

The oI phase probably corresponds to the monoclinic $\zeta 2$ phase with lattice parameters $a = 0.707$, $b = 0.408$, $c = 1.002$ nm, $\beta = 90.63°$ [16]. Although this monoclinic phase is nearly orthorhombic and its parameters are close to those of oI, there is no confusion in identifying the oI phase because monoclinic lattices cannot have the body-centered lattice type.

In order to determine if the $[001]_{oI,oF}$ twinning is 3- or 6-fold, bright-field images of the as-cast and annealed samples have been taken along the twinning axis $[001]_{oI,\ oF}$ (Figs. 6a and 6b). There are three oI twinning bands in Figure 6a as indicated by three arrows, each consisting of two twinning variants in the form of parallel strips. The angles between the bands are multiples of 60°. So we have in total six twinning variants, proving that the 3-fold twinning $120°/[001]_{oI}$ and the 2-fold twinning $180°/[310]_{oI}$ are present. The apparent 6-fold twinning in reciprocal space is only an artifact. The oF twinning modes are the same as those of the oI phase, *i.e.* the 3-fold twinning $120°/[001]_{oF}$ plus the 2-fold twinning $180°/[310]_{oF}$. Only two out of the three twinning bands of the oF phase are present in Figure 6a. In the annealed sample, the oF phase becomes the major component and six twinning variants are present as shown in Figure 6b.

The twinning modes of oF are shown schematically in Figure 7, where an hexagon is plotted inside the oF unit cell projected along the $[001]_{oF}$ direction, or 3-fold twinning axis. The lattice spots are represented by circles (lying on the projecting plane) and squares (lying at $c/2$ distance from the projecting plane). Six mirror planes

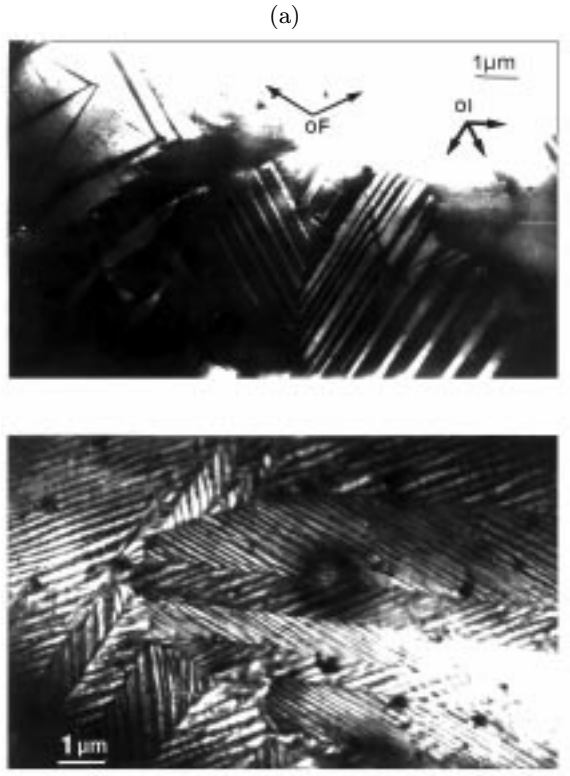

Fig. 6. Bright field images of the as-cast (a) and 500 °C/10 h annealed (b) samples taken along $[001]_{oF}$, oI. There are three oI twinning bands as indicated by three arrows in (a). Two oF twinning bands are present also in (a) while six oF variants in (b).

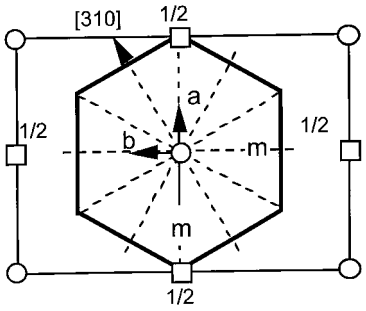

Fig. 7. One oF unit cell projected along $[001]_{oF}$ illustrating $120^\circ/[001]_{oF}$ and $180^\circ/[310]_{oF}$ twinning modes. Circles and squares are oF lattice points respectively on $z = 0$ and $z = 1/2$ layers. Thick lines outline a hexagonal unit cell of the $\varepsilon 2$ phase. The mirrors of the 6/mmm point group of $\varepsilon 2$ (in dotted lines) is transformed into two mirrors (marked by m) in the oF lattice, losing a 3-fold symmetry $120^\circ/[001]_{oF}$.

in hexagonal symmetry are drawn by dotted lines. The 2-fold twinning axis $[310]_{oF}$, perpendicular to the 3-fold twinning axis lies in one of the mirror planes.

The oF, oI and γ phases have coherent ORs. The diffraction patterns of two oF variants $[110]_{oF}$ and $[100]_{oF}$ in superposition with $[100]_{oI}$ of oI and $[110]_{\gamma}$ of γ are shown in Figure 8. Because of the twinning relationships, there are $6 \times 6 = 36$ equivalent ORs between oF and oI. The simplest OR is

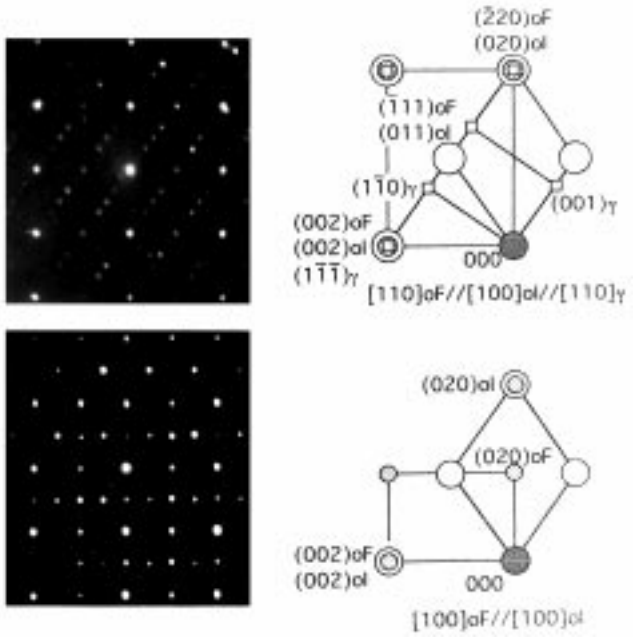

Fig. 8. Composite SAED patterns of oF, oI, and γ.

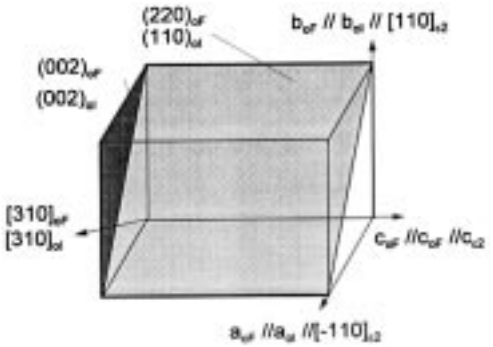

Fig. 9. Lattice relationships in the real space between oF, oI, and $\varepsilon 2$.

$(400)_{oF}//(200)_{oI}$, $(040)_{oF}//(020)_{oI}$, $(002)_{oF}//(002)_{oI}$, *i.e.* the basic axes a, b, and c are all parallel and $a_{oF} = 2 \times a_{oI}$, $b_{oF} = 2 \times a_{oI}$, $c_{oF} = c_{oI}$. Figure 9 illustrates this OR in real space. The OR between oF and γ can be expressed as: $(400)_{oF}//(110)_{\gamma}$, $(040)_{oF}//(\overline{112})_{\gamma}$, $(002)_{oF}//(\overline{111})_{\gamma}$.

4 Relationship between oF, oI and $\varepsilon 2$ phase

The twinning modes of oF and oI may suggest certain solid-state phase transitions from a high-temperature parent phase with higher symmetries. The twinning modes would correspond to the symmetries lost during such transitions. In the established phase diagram [9], there is a high-temperature phase $\varepsilon 2$, with the space group P63/mmc, that is located near the Al_3Cu_4 composition. Thus, we suppose that this phase may be the parent phase of oF and oI. The 6-fold axis of $\varepsilon 2$ would turn to a 2-fold (or a mirror) of oI or oF, losing a 3-fold symmetry ($120^\circ/[001]_{oF}$ and $120^\circ/[001]_{oI}$), and the mirror perpendicular to the 6-fold axis would be lost into the 2-fold twins in oF and oI ($180^\circ/[310]_{oF}$ and $180^\circ/[310]_{oI}$).

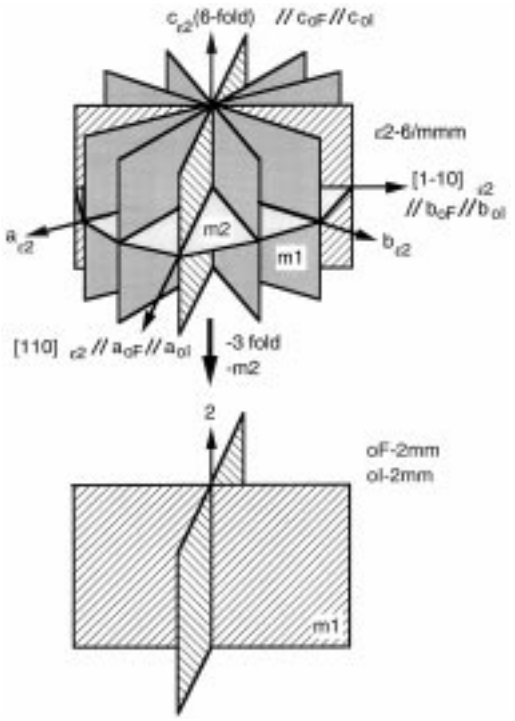

Fig. 10. Schematic illustration of the symmetry changes from the parent $\varepsilon 2$ phase with the 6/mmm point group (rank 24) to the product phases oF and oI, with the 2 mm point group (rank 4). The loss of the 3-fold and the mirror operations is recompensed by forming 3×2 twinning variants of the product phases.

According to the group-subgroup relationships, the rank of point group of the product phase multiplied by the number of variants is equal to the rank of point group of the parent phase. The point group 6/mmm of the $\varepsilon 2$ phase contains 24 symmetry operations. If oF and oI's point group is mmm, whose rank is 8, then there would be only three variants against six observed. So that only two point groups mm2 and 222 with rank of 4 are possible. Since the 2-fold twinning axis $[310]_{oF}$ lies perpendicular to the 6-fold axis of $\varepsilon 2$, the most probable point group should be mm2. The space groups for oF and oI are therefore Fmm2 and Imm2. Figure 9 illustrates also the ORs between the oF, oI and $\varepsilon 2$ phases. Figure 10 illustrates schematically the symmetry relationship between them.

Chemical compositions measured using EPMA are oF-$Al_{43}Cu_{57}$ and oI-$Al_{41.3}Cu_{58.7}$. The density of the smple is 5.58 ± 0.03 g cm^{-3}. If the two phases are supposed to have the same density, the number of atoms in their unit cells can be calculated: oF-$Al_{34.9}Cu_{46.3}$ and oI-$Al_{8.3}Cu_{11.7}$, which are approximately expressed as oF-$Al_{36}Cu_{48}$ and oI-Al_8Cu_{12}. As compared with their basic CsCl structure, the vacancy site number in their unit cells are respectively 12 for oF in 96 sites (12.5%) and 4 out of 24 sites for oI (16.7%), so that the unit cells are expressed by oF-$Al_{36}Cu_{48}\square_{12}$ and oI-$Al_8Cu_{12}\square_4$ ($\square$ representing a vacancy site).

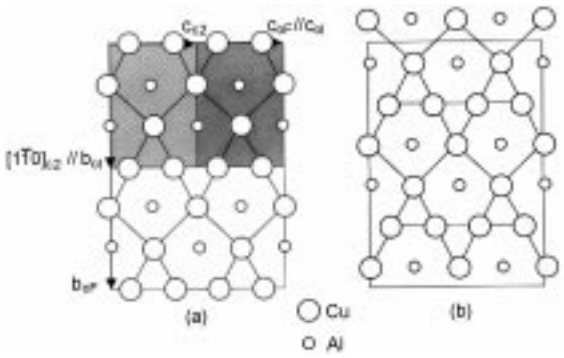

Fig. 11. Structural relationships between $\varepsilon 2$, oF, and oI. Two successive $\varepsilon 2$-(110) layers are shown in (a) and (b), where unit cells of the three phases and their parallel relationships are marked.

5 Approximant nature of $\varepsilon 2$, oF, and oI

Approximants are related to quasicrystals both by electronic structure (valence concentration) and atomic structure (characteristic subunits shared by all phases). Table 3 gives structural information and valence electron concentrations of oF, oI, $\varepsilon 2$, and i-AlCuFe. All these phases share similar valence electron concentrations per unit volume (N) and the criterion $2k_F \approx K$ is well satisfied. Therefore, the oF, oI, and $\varepsilon 2$ phases should all be regarded as approximants.

Approximants should contain structural information of corresponding quasicrystals. Apparently, these orthorhombic phases do not show any pseudo 5-fold or 10-fold symmetry in their electron diffraction pattern (in contrast to the fact that the Al-TM approximants exhibit strong diffraction spots nearly superposing those of corresponding quasicrystals). In our previous papers, we analyzed the approximant features of two B2-superstructures, namely Al_3Ni_2 [5] and γ-brass [6]. In both cases, diffraction patterns do not carry evident feature of quasicrystals (and this is why such phases have been ignored for a long time). However, in their atomic structures, icosahedral or pentagonal networks are easily recognizable. It seems to be a general property for the B2-based approximants that their strong diffraction spots superpose only partially those of quasicrystals but they do contain structural information of the latter. The oF, oI, and $\varepsilon 2$ phases are also B2-superstructures. The difficulty in this case is that the atomic structures of oF and oI are unknown.

It is difficult to resolve the atomic structures of oF and oI because the samples contain always a mixture of at least these two phases (small amount of γ-brass is present). However, we can refer to the $\varepsilon 2$ structure in order to get an intuitive idea of the oF and oI structures.

The orientation relationships of $\varepsilon 2$ with respect to oF and oI are: $c_{\varepsilon 2}$ // c_{oF} // c_{oI}, $[110]_{\varepsilon 2}$ // $a_{oF}/2$ // a_{oI}, $[1\bar{1}0]_{\varepsilon 2}$ // $b_{oF}/2$ // a_{oI}, as shown in Figure 9. These relationships are shown again in Figures 11a and 11b, where oI and oF cells are marked on two successive $(110)_{\varepsilon 2}$ layers of $\varepsilon 2$. This plane is parallel to a $\{110\}_{B2}$ of the basic B2 lattice. This plane is also perpendicular to the 5- or 10-fold axis of quasicrystals. A distinct feature of approximants is noted: deformed pentagons in these planes form

Table 3. Structural information of the oF, oI, $\varepsilon 2$ and i-AlCuFe phases.

Composition (at%)	Number of atoms per nm^3	valence electron number per atom (e/a)	valence electron number per nm^3 (N)	$2k_F$ (nm^{-1})	$k_{intense}$ (nm^{-1})
oF-Al_3Cu_4	69.3	1.86	128.9	31.3	30.8
oI-Al_2Cu_3	69.3	1.80	124.7	30.9	30.8
$\varepsilon 2$-Al_2Cu_3	71.6	1.74	124.7	30.9	30.4, 30.3
i-$Al_{62.3}Cu_{24.9}Fe_{12.8}$	66.7	1.86	124.1	30.9	31.4, 29.9

a network that resembles the local atomic configurations in the 5-fold or 10-fold planes of quasicrystals. The $(110)_{\varepsilon 2}$ cross-section of one $\varepsilon 2$ unit cell (or the $[110]_{\varepsilon 2}$ projection) contains two pentagonal subunits plus one thin rhombus subunit. The two $(110)_{\varepsilon 2}$ planes are the same but displaced along $[1\bar{1}0]_{\varepsilon 2}$ by $[1\bar{1}0]_{\varepsilon 2}/2$. Along the $[110]_{\varepsilon 2}$ direction the pentagons are aligned into pentagonal chains. The [100] projections of oF and oI comprise respectively 8 pentagons plus 4 rhombi and 4 pentagons plus 2 rhombi.

6 Conclusions

As indicated by the e/a-constant line theory, possible Al-Cu approximants should be located near composition Al_3Cu_4. We have found two new phases in this alloy: oF-$Al_{432}Cu_{56.8}$ and oI-$Al_{41.3}Cu_{58.7}$. Their space groups are probably oF-Fmm2 and oI-Imm2. Their e/a ratios are the same as that of the Al-Cu-Fe icosahedral quasicrystal. Both are B2 vacancy-containing superstructures; unit cell compositions can be expressed approximately as oF-$Al_{36}Cu_{48}\square_{12}$ and oI-$Al_8Cu_{12}\square_4$ ($\square$: vacancies). They both exist in twinning variants of the types $120°/[001]_{oF}$ and $120°/[001]_{oI}$ (*i.e.* 3-fold twinning) and $180°/[310]_{oF}$ and $180°/[310]_{oI}$ (*i.e.* 2-fold twinning). These twinning modes are explained by solid-phase transitions from their high-temperature hexagonal phase $\varepsilon 2$. The $\varepsilon 2$ phase contains obvious pentagonal atomic networks. After analyzing their valence electron concentrations and atomic structure features, we arrive at the conclusion that the oF, oI and $\varepsilon 2$ phases are all B2-based approximants of the Al-Cu-TM quasicrystals.

Appendix

If two variants or two phases ($t1$ and $t2$) satisfy an OR defined by three pairs of independent superposing lattice planes $(h_1k_1l_1)_{t1}//(h_1k_1l_1)_{t2}$, $(h_2k_2l_2)_{t1}//(h_2k_2l_2)_{t2}$ and $(h_3k_3l_3)_{t1}//(h_3k_3l_3)_{t2}$, the OR in terms of the reciprocal basic vectors a^*, b^* and c^* can be expressed as:

$$\begin{bmatrix} a^* \\ b^* \\ c^* \end{bmatrix} = \begin{bmatrix} h_1\ k_1\ l_1 \\ h_2\ k_2\ l_2 \\ h_3\ k_3\ l_3 \end{bmatrix}_{t2}^{-1} \cdot \begin{bmatrix} h_1\ k_1\ l_1 \\ h_2\ k_2\ l_2 \\ h_3\ k_3\ l_3 \end{bmatrix}_{t1} \cdot \begin{bmatrix} a^* \\ b^* \\ c^* \end{bmatrix}_{t1} = \begin{bmatrix} a_{11}\ a_{12}\ a_{13} \\ a_{21}\ a_{22}\ a_{23} \\ c_{31}\ c_{32}\ c_{33} \end{bmatrix}_{t1} \cdot \begin{bmatrix} a^* \\ b^* \\ c^* \end{bmatrix}_{t1} = \mathrm{M} \begin{bmatrix} a^* \\ b^* \\ c^* \end{bmatrix}_{t1}. \quad (1)$$

The matrix M represents the OR between $t1$ and $t2$. When $t1$ and $t2$ are two variants (or grains) of one phase, this matrix signifies a pure rotation of θ angle along a certain $[uvw]_{t1}$ direction. The angle θ is calculated by $\arccos((a_{11} + a_{22} + a_{33} - 1)/2)$. For orthorhombic lattices, the directional indices of the rotation axis is expressed as $u : v : w = (a_{32} - a_{23})/a : (a_{13} - a_{31})/b : (a_{21} - a_{12})/c$ for $\theta \neq 180°$, and $u : v : w = (\sqrt{a_{11} + 1}/a : \sqrt{a_{22} + 1}/b : \sqrt{a_{33} + 1}/c$ for $\theta = 180°$, where a, b and c are the orthorhombic lattice constants [15]. The zone axis $[uvw]$ and the plane indices (hkl) are mutually transformed by equations for an orthorhombic lattice.

References

1. W. Steurer, Z. Krist. **190**, 179 (1990).
2. A.P. Tsai, A. Inoue, T. Masumoto, Jpn J. Appl. Phys. **26**, L1505-7 (1987).
3. C. Dong, Y.C. Fu, D.H. Wang, W.M. Xu, M.L. Song, Y.M Wang, J. Mater. Res. Chn. **9**, 107 (1994) (in Chinese).
4. C. Dong, *Proceedings of the 5th Int. Conf. on Quasicrystals* (ICQ5), Avignon, 1995, edited by C. Janot, R. Mosseri (World Scientific, 1996), p. 334.
5. C. Dong, J. Phys. France I **5**, 1625 (1995).
6. C. Dong, Phil. Mag. A **73**, 1519 (1996).
7. C. Dong, A. Perrot, J.M. Dubois, E. Belin, Maters. Sci. Forum **150-151**, 403 (1994).
8. C. Dong, Scripta Metall. Mater. **33**, 239 (1995).
9. J.L. Murray, Int. Metals Rev. **30**, 211 (1985).
10. M. El-boragy, R. Szepen, K. Schubert, J. Less-Common Metals **29**, 133 (1972).
11. A.J. Bradley, P. Jones, J. Inst. Metals **51**, 131 (1933).
12. L. Arnberg, S. Westman, Acta Crystallogr. A **34A**, 339 (1978).
13. P. Villars, L.D. Calvert, *Pearson's Handbook of Crystallographic Data for Intermetallic Phases* (Materials Park, OH 44073, 1985).
14. G.V. Raynor, *Annotated Equilibrium Diagrams*, No. 4 (The Institute of Metals, London, 1944).
15. V. Randle, *The Measurement of Grain Boundary Geometry* (The Institute of Physics Publishing, Bristol and Philadelphia, 1993).
16. A.J. Bradley, H.J. Goldschmidt, J. Inst. Metals **65**, 389 (1939).